Ritesh Singh
Research Scholar
University of Petroleum & Energy Studies
Department of Aerospace Engineering
Dehradun, Uttarakhand, 248007
India

Assistant Professor
Manipal University Jaipur
Department of Electrical Engineering
Jaipur, Rajasthan, 303007
India

Om Prakash
Professor
University of Petroleum & Energy Studies
Department of Aerospace Engineering
Dehradun, Uttarakhand, 248007
India

Sudhir Joshi
Professor
Graphic Era (Deemed to be University)
Department of Mechanical Engineering
Dehradun, Uttarakhand, 248002
India

Control Design Using PID with State Feedback for Air-Breathing Hypersonic Vehicle

The paper uses the state feedback technique to provide a control design method for a dynamic linear 6-degree-of-freedom (DOF) model of an Air-breathing Hypersonic Vehicle (AHV). A linear model of AHV with a state space model is developed for the open loop simulation for the level flight with Mach number 5 and a height of 65000 ft (19812 m). The dynamic stability of AHV is analyzed, and state feedback with the pole placement method is implemented for the controller design. The dynamic stability, response, and comparison for the PI and PID controller are presented for the aileron deflection δ_a and rudder deflection δ_r for the AHV linear model.

Keywords: *PID, State Feedback, Hypersonic Vehicle, Air-breathing Hypersonic Vehicle, 6DOF Simulation, Linear Hypersonic Model*

1. INTRODUCTION

The hypersonic technology with air-breathing capa–bilities proves an economical solution for routine space access. Its rapid space transportation from Earth to Space is widely used for civilian and military appli–cations. International attention to future possibilities of Hypersonic has resulted in extensive research of Hypersonic Technology worldwide for military and civilian uses. Traveling large distances with high speed and cost-effectively using Air-breathing Hypersonic Vehicle (AHV) in Low Earth Orbit is possible. A renewed interest in Hypersonic Vehicles has grown with the demand for high-quality, low-cost space travel using AHVs. Considering practical applicability, military and commercial applications and Single Stage To Orbit (SSTO) missions utilizing AHV technology has enormous promise for Space tourism.

AHV dynamics and control are major concerns with the Flight Control Systems (FCS) design due to the dynamic behavior and extremely coupled nonlinear nature. AHVs control design should provide stability to the FCS and, consistent performance and robustness, as AHVs are enormously subtle to atmospheric conditions and aerodynamic parameters. Control design performance is difficult to achieve with the best performance with all the flight regimes and conditions, so the control design schemes must be adaptive. In the hypersonic flight analysis for control design, models like the longitudinal dynamics model, control-oriented model, and 6-degree-of-freedom (DOF) rigid-body models are used for the stability and controller design and to model uncertainty and non-minimum phase occurrence. Hypersonic vehicles' aerodynamic challenges and difficulties explain various aerodynamic phenomena occurring at different altitudes at the hypersonic speed of flight. There are several challenges with AHV hypersonic flight because of the wide flying envelope and dynamic interaction between different Mach speeds. This necessitates the dynamic and control analysis of AHV with flight dynamics and stability analysis.

Challenges in the design of controllers in [1] for the AHVs have multidisciplinary involvement of the materials, aerodynamics, flight mechanics, automatic control, artificial intelligence, and computer, is outlined. It discusses the control issues focusing on the complete maneuver control of AHVs in widespread flight envelop involving the climbing, cruising, re-entry, and inter-shifting regimes stages of the flight trajectory. The flight control design involves typical aspects such as coupling and control constraints, non-minimum phase, flexible modes, robust intelligent and integrated control design, mixed engine configuration, aerodynamic effects, and flight test data. These are the typical issues raised in [1]. Intelligent control techniques can be designed to provide robust flight control using optimization techniques, offering assured stability for AHVs. Design techniques and stability for control are in the research phase, and many more analyses are still developing for the AHVs.

For many reasons, the flight control problem for hypersonic vehicles goes far beyond the difficulties encountered with the previous aircraft and spacecraft designs. The control obstacles, such as with the other high-performance aircraft like hypersonic vehicle dynamics, exhibit a nonlinear, multivariable, time-varying, non-minimum phase type of behavior. Most of the analysis will have to be best approximated so that AHVs FCS may have to operate using a simplified system model, including some parameters uncertain. This paper presents the 6DOF linear model analysis for the linearized aerodynamic model of the selected Mach number *M=5* for the AHV flying envelope. The linear-ized 6DOF dynamic model uses linear aerodynamic, thrust engine, and standard atmospheric developed model for developing a linear 6DOF simulation model.

Received: January 2023, Accepted: April 2023
Correspondence to: Ritesh Singh
Department of Electrical Engineering,
Manipal University Jaipur, Rajasthan, 303007, India
E-mail: ritesh.singh23@gmail.com
doi: 10.5937/fme2302221S

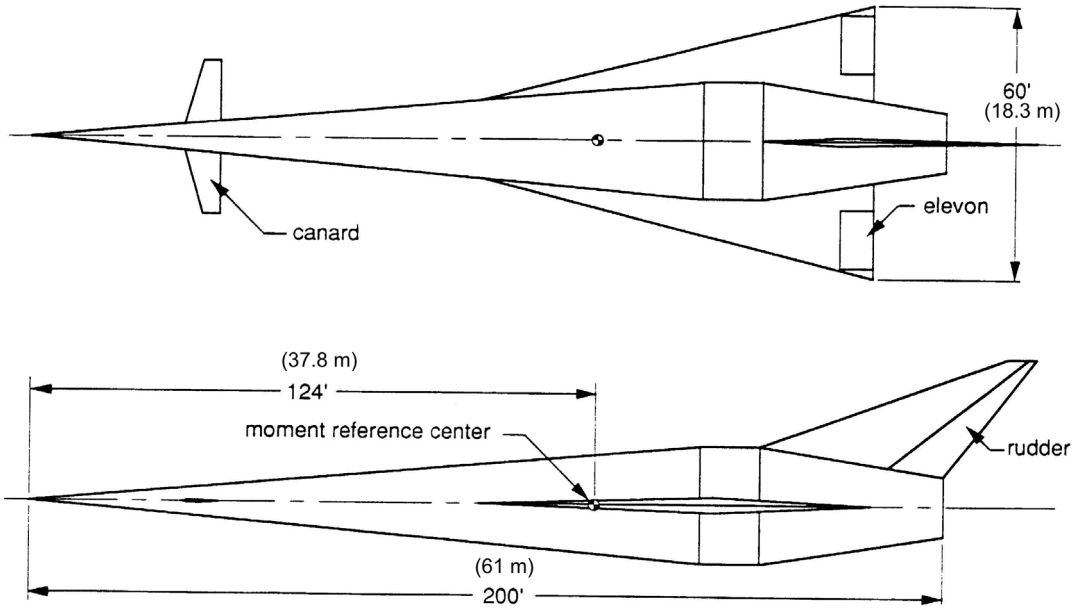

Figure 1. AHV model [7]

The developed 6DOF linear simulation model is used for the open loop and stability analysis and to understand the dynamic behavior using pole-zero location and its stability.

Further controller design techniques can be imple–mented. Further state feedback approach is used to analyze open loop and closed loop responses of the linear 6DOF dynamic AHV model, indicating closed-loop stability for AHV. The controller design [2] is carried out with state feedback design using linear control law design [3,4] using pole placement [5], and controllers like Proportional Integral (PI), Proportional Derivative (PD), and Proportional-Integral-Derivative (PID) are considered for controller development [6] for AHVs. The linear controller is designed for the AHV for different control inputs, and stability is analyzed for the considered level flight condition. The work is an extension of the work presented in [24].

The sections are presented for the paper with the following structure. AHV dynamics with nonlinear flight dynamics, aerodynamics coefficient, thrust engi–nes, and atmospheric conditions are presented in Section 2. Section 3 addresses the control design using the state feedback technique for the considered AHV dynamics. Section 4 outlines the simulation for open loop dynamic simulation of the 6DOF AHV linear model and dis–cusses the stability for Mach number, M=5, and also shows the control law implemented to the linear dynamic 6DOF AHV linear model and pre-sents the result for the different controller implemented like PI and PID using state feedback design. Section 5 finally illustrates and presents the conclusion.

2. AHV MODEL DEVELOPMENT

The winged Cone model, GHV (Generic Hypersonic Vehicle), built with NASA Langley Research Centre [7], shown in Figure 1, is selected for the analysis and design using the state control feedback approach. The propulsion system is hypothetical proposed with group alignment of turbojet, ramjet, and scramjet, and with rocket propulsion system [8], are incorporated into the model. Center-of-mass, center-of-gravity, and moment-of-inertia are included with the model motion of equations for simulation. Fuel consumption affects the vehicle's weight, center-of-gravity, and inertia products. *The X*-axis of the body is completely aligned with the vehicle's thrust vector orientation. As a result, there is no thrust force component in the body (*Y* and/or *Z*-axis). Due to this, it is expected that when fuel is spent, the center of gravity will individually shift beside the body's *X*-axis. Axis symmetrical modeling is used to create the winged cone model, and the axis of rotation is parallel to the model's wing tips and tail. The AHV control surfaces are the elevon (left and right), canard, and rudder. They are tested for elevator deflections in relation to hinge lines and rudder deflections with the trailing edge. The canards are either ignored or regarded as ineffectual at high AHV speeds. The mathematical modeling of the AHV model uses the flat Earth approximation, and equations of motion are established with Newton and Euler equations. AHV model geometrical specifications are used from [9].

The AHV 6DOF modeling uses the flat Earth approximation and thrust assembly inclines with the body *X* axis, and with *Y* and *Z* axes are free with Thrust force (F_{Tx}). The 6DOF dynamic model of AHV [9] is provided by (1)-(9),

$$m\dot{u} = rv - qv - g\sin\theta + F_{ax} + F_{Tx} \tag{1}$$

$$m\dot{v} = pw - rv + g\cos\theta + F_{ay} \tag{2}$$

$$m\dot{w} = qu - pv + g\cos\theta + F_{az} \tag{3}$$

$$\dot{p} = c_1 qr + c_2 pq + c_3 L_a + c_4 N_a \tag{4}$$

$$\dot{q} = c_5 pr - c_6\left(p^2 - q^2\right) + c_7 M_a \tag{5}$$

$$\dot{r} = c_8 pq - c_2 qr + c_4 L_a + c_9 N_a \tag{6}$$

$$\dot{\phi} = p + q\sin(\phi)\tan(\theta) + r\cos(\phi)\tan(\theta) \tag{7}$$

$$\dot{\theta} = q\cos\phi - r\sin\phi \tag{8}$$

$$\dot{h} = u\sin\theta - v\sin(\phi)\cos(\theta) - w\cos(\phi)\cos(\theta) \tag{9}$$

the body axis components of AHV velocities u, v, and w are related to the Earth axis, and $\dot{u}$, $\dot{v}$ and $\dot{w}$ are the corresponding acceleration along body X axis, Y axis and Z axis; and p, q and r are angular velocities with $\dot{p}$, $\dot{q}$ and $\dot{r}$ as angular rates; F_{ax}, F_{ay} and F_{az} are body-axis components for aerodynamic forces of AHV and L_a, N_a and M_a are the body-axis component of aerodynamic-moment affecting AHV. The Euler angles as roll angle and the pitch angle are given by ϕ and θ, and their derivatives as $\dot{\phi}$ and $\dot{\theta}$, and here m and h are AHV mass and altitude. Considered inertial components c_1 to c_9 are constant moments of inertia from [9].

AHV dynamics (10)-(12) is obtained in the wind axis and is given for velocity, angle-of-attack and sideslip angle with V, α, and β followed by their rates.

$$\dot{V} = \frac{1}{V}\left(u\dot{u} + v\dot{v} + w\dot{w}\right) \tag{10}$$

$$\dot{\alpha} = \frac{\left(u\dot{w} - w\dot{u}\right)}{\left(u^2 + w^2\right)} \tag{11}$$

$$\dot{\beta} = \frac{\left[\left(u^2 + w^2\right)\dot{v} - v\left(u\dot{u} + w\dot{w}\right)\right]}{\left(V^2\sqrt{u^2 + w^2}\right)} \tag{12}$$

Relationship between components is shown as: $u=V\cos(\alpha)\cos(\beta)$, $v=V\sin(\beta)$, $w=V\sin(\alpha)\cos(\beta)$, $V = |V| = \sqrt{u^2 + v^2 + w^2}$ with angles given as, $\alpha = \tan^{-1}(w/u)$ and $\beta = \sin^{-1}(v/V)$

The nonlinear aerodynamic coefficient of AHV from [10] is linearized for the 6DOF linear model simulation considering at Mach number, M=5. The linearized equations for the dynamic simulation of the linear AHV model are obtained using an analytical method considering fixed points for linearization and ignoring the higher terms. Hence, the reduced linearized aerodynamic coefficient model is obtained by (13)-(18).

$$C_L = C_{L,\alpha} + C_{L,\delta_e}\delta_e \tag{13}$$

$$C_D = C_{D,\alpha} + C_{D,\delta_e}\delta_e \tag{14}$$

$$C_m = C_{m,\alpha} + C_{m,\delta_e}\delta_e + C_{mq}\left(\frac{qc}{2V}\right) \tag{15}$$

$$C_Y = C_{Y,\beta}\beta + C_{Y,\delta_a}\delta_a + C_{Y,\delta_r}\delta_r \tag{16}$$

$$C_l = C_{l,\beta}\beta + C_{l,\delta_a}\delta_a + C_{l,\delta_r}\delta_r + C_{lr}\left(\frac{rb}{2V}\right) + C_{lp}\left(\frac{pb}{2V}\right) \tag{17}$$

$$C_n = C_{n,\beta}\beta + C_{n,\delta_a}\delta_a + C_{n,\delta_r}\delta_r + C_{nr}\left(\frac{rb}{2V}\right) + C_{np}\left(\frac{pb}{2V}\right) \tag{18}$$

Aerodynamics coefficient, and dynamics from [10], [11], are implemented to develop an aerodynamic model of total lift coefficient, drag coefficient, pitching moment coefficient, side force coefficient, rolling moment coefficient, yawing moment coefficient as C_L, C_D, C_m, C_Y, C_l, and C_n respectively, and is given using (13-18) considering entire flight envelops of AHV. Interpolation is performed by creating subroutines of the aerodynamic data, and the aerodynamic coefficients are determined. Aerodynamic force represented by lift force is described with $L = \bar{q}SC_L$ drag force represented with $D = \bar{q}SC_D$, side force expressed with $Y = \bar{q}SC_Y$, the rolling moment as $L_a = \bar{q}S_bC_l$ the pitching moment is expressed as $M_a = \bar{q}S_cC_m$, and yawing moment is given by $N_a = \bar{q}S_bC_n$ Here $\bar{q}$, S, b, c is the dynamic pressure, reference area, span and mean aerodynamic chord respectively. The linear aerodynamic coefficient equations of the 6DOF dynamic simulation model of AHV are given by (13)-(18). Here the control surfaces of AHV are given by δ_e, δ_a, and δ_r as elevator, aileron, and rudder deflection. The elevon (left and right) relation to aileron and elevator deflection is developed using the relation as $\delta_{left\_e}=\delta_a+\delta_e$ and $\delta_{right\_e}=-\delta_a+\delta_e$. The increment derivatives are given by the notation $C_{L,\alpha}$ and $C_{L,\delta e}$ for lift, and similarly expressed for drag, pitching moment, side force, rolling moment, and yawing moment, and here V is AHV free stream velocity.

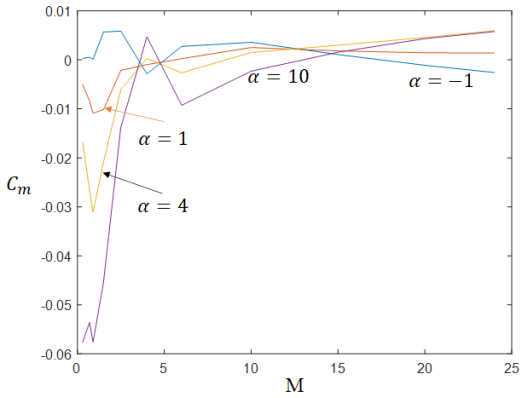

Figure 2. Aerodynamic coefficient of C_m versus M [11,12]

The aerodynamic pitching coefficient C_m of AHV is shown in Figure 2 with the Mach number M variation for the complete flight regime *M=0 to 24.*

The proposed propulsion incorporates a theoretical ramjet and scramjet engine. The thrust engine model [10-12] is used over a wide variety of flight envelopes. Considering the 6DOF model, AHV engine dynamics using (19) is implemented with Mach number, height, and PLA (pilot-lever-angle), and a function with selected flight envelop of M=5.

$$\begin{aligned} T_{\text{ramjet}} = \text{PLA}(&7.53\times10^2\times M^7 - 1.5\times10^4\times M^6 + \\ &+1.16\times10^5\times M^5 - 4.36\times10^5\times M^4 + \\ &+8.07\times10^5\times M^3 - 6.97\times10^5\times M^2 + \\ &+3.94\times10^5\times M + 3.93\times10^{-8} \end{aligned} \tag{19}$$

Mach numbers with related altitude changes need an atmospheric model that includes temperature and density data. As the temperature and density of the air are affected by the height disparity, the relation is given by (20) and (21) for height, h≥36089 *ft* (11000 *m*).

$$\rho = 0.2971\rho_0 e^{-\frac{(h-36089)}{20806.7}} \tag{20}$$

$$\rho_0 = 2.377\times10^{-3}\,\text{slug/ft}^3 \tag{21}$$

The dynamic model for simulation using (10)-(12) and (4)-(9) is used to obtain the AHV model given by

the states $[V,h,\alpha,\theta,q,T,\beta\ \phi,\ p,r]^{T}$ Considering the nonli–near AHV model given by (10)-(12) and (4)-(9) are linearized using small disturbance theory by [13], and with steady and wing level flight and with no sideslip, is considered as reference condition with the steady and perturbated state. The linearized model derived here with the longitudinal and lateral dynamics models is decoupled from each other. The linear model obtained here is considered for the case of level and straight flight at fixed velocity and altitude, considering the bank angle as zero. The linear AHV model is expressed with the state space design approach [14] and the model is represented by (22)-(23), and here A_n is the normal acceleration of the AHV; pitch rate and angle of attack are given by q and α. The states, input, and output are given by (24)-(26).

$$\dot{x} = Ax + Bu \tag{22}$$

$$Y = Cx + Du \tag{23}$$

$$x = \left[V\ h\ \alpha\ \theta\ q\ T\ \beta\ \phi\ p\ r\right]^{T} \tag{24}$$

$$u = \left[PLA\ \ \delta_a\ \ \delta_e\ \ \delta_r\right]^{T} \tag{25}$$

$$Y = \left[A_n\ \ q\ \ \alpha\right]^{T} \tag{26}$$

3. CONTROL DESIGN USING STATE FEEDBACK

The controller design aspects for the AHVs from the control law design point of view using the state feed–back approach [15] are presented here. There is a strong correlation between the closed-loop stability of the Linear Time-Invariant (LTI) system and the location of the system's poles. As a result, while designing a closed-loop system, the poles placed should have reasonable and anticipated performance. The pole-placement met–hod uses state or output feedback to locate the poles at the required location. Pole placement is critical in system design since system performance is directly related to pole placements. Two primary steps must be followed. The placement or assignment of poles is the initial stage, followed by determining feedback using gain values. The system's control is required and adequate for the state feedback-based strategy using the closed-loop pole placement method.

Controllability is a critical quality to test before using our state-space controller design methodologies [16,17]. There must be a controllability attribute in order for us to influence the system's current state. The system's closed-loop poles may be located anywhere on the s-plane. The controllability matrix given by (27) must be satisfied for the system to state controllable fully,

$$\boldsymbol{P} = [\boldsymbol{B}\ \ \boldsymbol{AB}\ \ \boldsymbol{A}^2\boldsymbol{B}\ \ \ldots\ \ \boldsymbol{A}^{n-1}\boldsymbol{B}] \tag{27}$$

and should have rank n. The number of rows in a matrix determines its rank (or columns), and the system has n state variables, where n is the state variables count.

The state-space method with the state feedback technique offers more appropriate control design constraints considering movement with complete closed-loop poles autonomously to one another. A controller with full-state feedback creates the input vector $u(t)$, and accordingly, the control law is designed with state-space representation. Considering the control law design using the state feedback method, the LTI system state model expressed with (22-23), indicating open-loop dynamics representation needs controller design. For the state feedback-based design control law using the state model is expressed using (28),

$$\boldsymbol{u}(t) = -\boldsymbol{K}\boldsymbol{x}(t) + \boldsymbol{r}(t) \tag{28}$$

where the dimension of K is $m'n$, and to accomplish required system attributes with a feedback approach, the state-run equations are expressed using (29),

$$\dot{x}(t) = (A - BK)x(t) + Br(t) \tag{29}$$

and the block diagram depiction of (29) is represented and given in Figure 3.

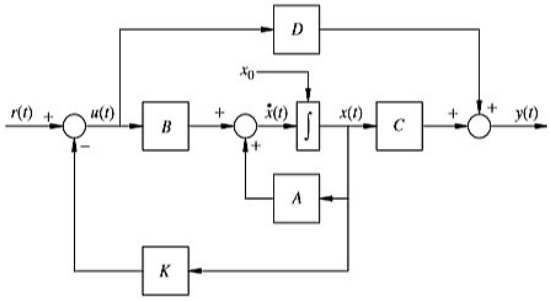

Figure 3. Model closed-loop state feedback control

Transfer function from state space representation is presented and given by (30),

$$\boldsymbol{G} = \boldsymbol{C}(s\boldsymbol{I} - \boldsymbol{A})^{-1}\boldsymbol{B} + \boldsymbol{D} \tag{30}$$

with the characteristics polynomial for the system is expressed and provided using (31).

$$\left|sI - (A - BK)\right| = 0 \tag{31}$$

Considering a symmetric set of n complex values given by $(\mu_1, \mu_2, \ldots, \mu_n)$ indicating considered closed-loop eigenvalues of the system, hence desired closed-loop characteristics polynomial is given by (32).

$$\alpha(s) = (s - \mu_1)(s - \mu_2)\ldots(s - \mu_n) = s^n + \alpha_{n-1}s^{n-1} + \ldots + \alpha_2 s^2 + \alpha_1 s^1 + \alpha_0 \tag{32}$$

For determining the state feedback gain **K**, Ackermann's formula is used and considering closed-loop characteristics polynomial $\alpha(s)$, and the gain of the state feedback is expressed using (33),

$$\boldsymbol{K} = [0\ \ 0\ \ \ldots\ \ 0\ \ 1]\boldsymbol{P}^{-1}\boldsymbol{\alpha}(\boldsymbol{A}) \tag{33}$$

where **P** gives the controllability matrix, and cont–rollable pair (**A**, **B**) and **α**(**A**) gives $n'n$ matrix given by (34).

$$\alpha(A) = \boldsymbol{A}^{n} + \alpha_{n-1}\boldsymbol{A}^{n-1} + \ldots + \alpha_2\boldsymbol{A}^2 + \alpha_1\boldsymbol{A}^1 + \alpha_0\boldsymbol{I} \tag{34}$$

The state feedback can be designed with the gain matrix to achieve desirable closed-loop eigenvalues. As shown in Figure 4, it can be implemented using a state-space model demonstration with desired control.

Linear state feedback control law design with pole placement is used in the control design for the AHV model, and the controller is implemented and is compared to those obtained with other controllers like

proportional-integral (PI) controller and proportional-integral-derivative (PID) [18]. State realization using the feedback version for the feedback-based controller design is realized using (30). It is modeled using a closed-loop state equation with pole positioning to achieve the required performance attributes.

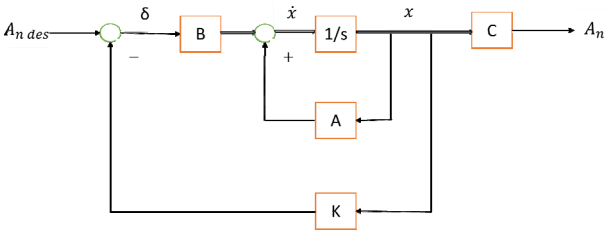

Figure 4. State model representation with the desired control

4. SIMULATION AND RESULTS

The developed linear 6DOF AHV model given by (22-23) is used for the simulation to understand the open loop dynamic behavior and the model's response. The simulation incorporates the aerodynamic coefficient model, the engine model with the propulsion engine, and with the standard atmospheric conditions from Section 2. The AHV model simulation is carried out for the M=5 Mach number and h=65000 ft (19812 m) altitude with level flight conditions.

4.1 Open Loop Dynamic Simulation

The state variables given by (24) are determined for the M=5, and the state space model matrices are obtained as **A**, **B**, **C**, and **D**. This model is obtained considering the level and straight AHV flight for considered velocity as M=5 and height of 65000 ft (19812 m) considering the banking angle of zero. The model obtained is decoupled from the longitudinal and lateral system interactions. The linearized models **A**, **B**, **C**, and **D** are obtained for the AHV model considering trimmed for M=5 and height of 65000 ft (19812 m).

$$\mathbf{A}=\begin{bmatrix} 0 & 0 & -6.238 & -0.0312 & 0 & 0 & 0 & 0 & 0 & 0 \\ 0.0002 & 0 & -4.851 & 4.851 & 0 & 0 & 0 & 0 & 0 & 0 \\ 0 & 0 & -0.0002 & 0 & 0.001 & 0 & 0 & 0 & 0 & 0 \\ 0 & 0 & 0 & 0 & 0 & 0 & 0 & 0 & 0 & 0 \\ 0 & 0 & -0.0125 & 0 & 0 & 0 & 0 & 0 & 0 & 0 \\ 0 & 0 & 0 & 0 & 0 & 0 & 0 & 0 & 0 & 0 \\ 0 & 0 & 0 & 0 & 0 & 0 & -0.0001 & 0 & 0 & -0.001 \\ 0 & 0 & 0 & 0 & 0 & 0 & 0 & 0 & 0.001 & 0.0002 \\ 0 & 0 & 0 & 0 & 0 & 0 & -0.0023 & 0 & 0 & 0 \\ 0 & 0 & 0 & 0 & 0 & 0 & 0.0005 & 0 & 0 & 0 \end{bmatrix}$$

$$\mathbf{B}=\begin{bmatrix} 36.92 & -0.0029 & 0 & 0.0016 \\ 0 & 0 & 0 & 0 \\ -0.0003 & 0.0001 & 0 & 0 \\ 0 & 0 & 0 & 0 \\ 0 & 0.0018 & 0 & 0 \\ 0 & 0 & 0 & 0 \\ 0 & 0 & 0 & 0.0001 \\ 0 & 0 & 0 & 0 \\ 0 & 0 & -0.0056 & 0.0047 \\ 0 & 0 & 0 & -0.0021 \end{bmatrix}$$

$$\mathbf{C}=\begin{bmatrix} 0.0003 & -0.0524 & -12.48 & 0 & 0 & 0 & 0 & 0 & 0 & 0 \\ 0 & 0 & 0 & 0 & 1 & 0 & 0 & 0 & 0 & 0 \\ 0 & 0 & 57.3 & 0 & 0 & 0 & 0 & 0 & 0 & 0 \end{bmatrix}$$

$$\mathbf{D}=\begin{bmatrix} 0 & -0.0107 & 0 & -0.0107 \\ 0 & 0 & 0 & 0 \\ 0 & 0 & 0 & 0 \end{bmatrix}$$

The open loop dynamic simulation is carried out for the output state space model given by (26) and the corresponding inputs from aileron and rudder deflec–tions using (25).

The open loop dynamic analysis shows the stability concerns using Bounded Input Bounded Output (BIBO) condition [19] for the simulated flight behavior. For the δ_a deflection, A_n shows unstable behavior, and α and q remain stable for the considered flight condition, as shown in Figure 5. Similarly, for the δ_r deflection, A_n, q, and α results in the unstable behavior of the AHV flight, as shown in Figure 6. Therefore, AHV flight for the considered state must be stabilized for the δ_a and δ_r deflection, using controller design and closed-loop analysis for all outputs.

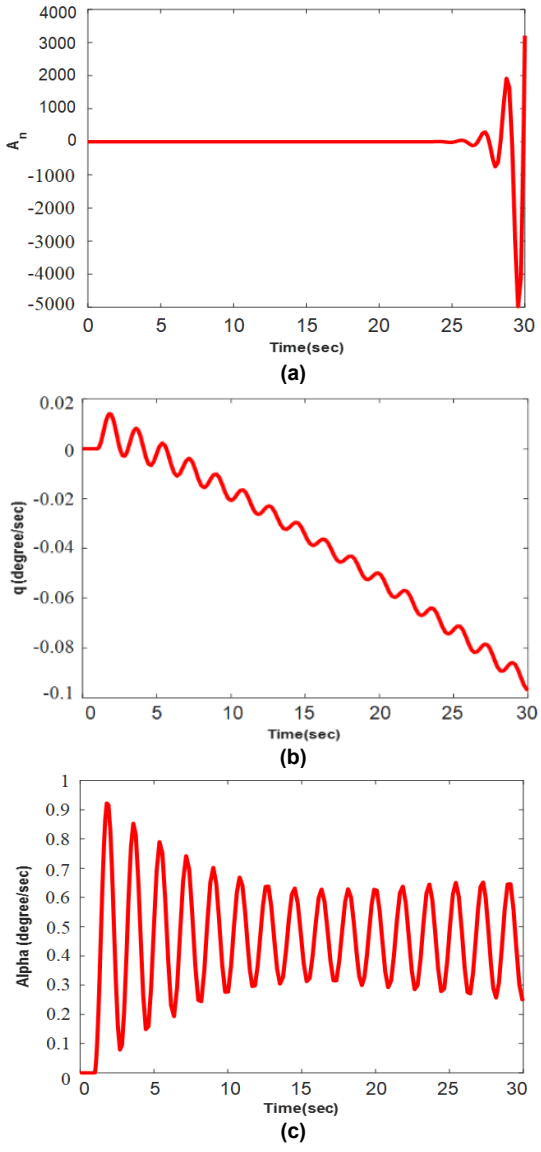

Figure 5. Response for elevator deflection δ_a

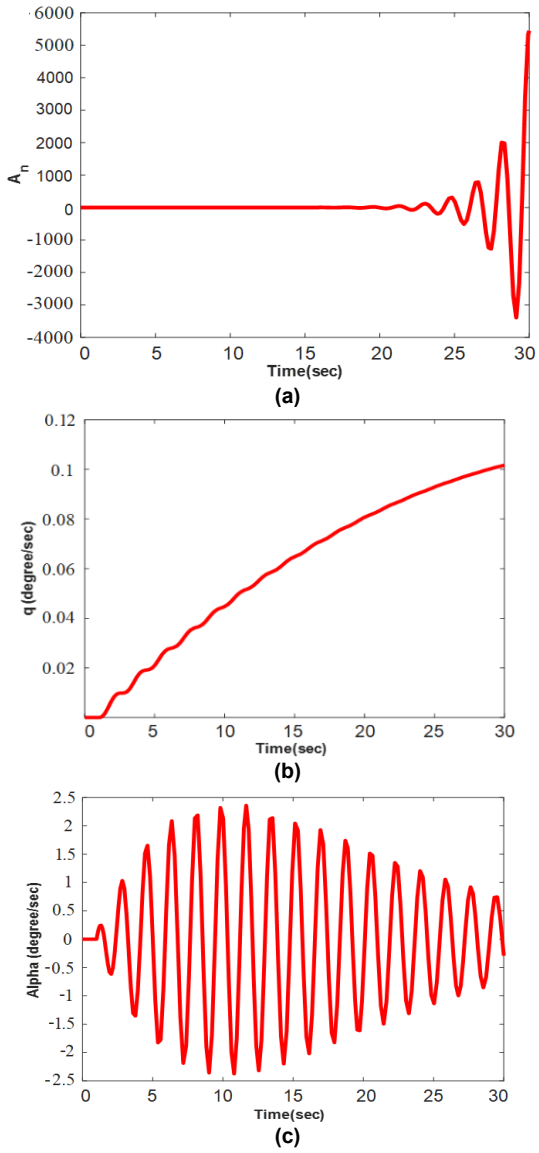

Figure 6. Response for rudder deflection δ_r

The pole-zero plot of the model demonstrates the recurrence of poles and zeros on the RHS plane, denoting the nonminimum phase for the AHV, as shown in Figure 7. As a result of these nonminimum phases [20,21], which render the system unstable, the AHV model flight circumstances for the anticipated level flight at M=5 Mach number are unstable.

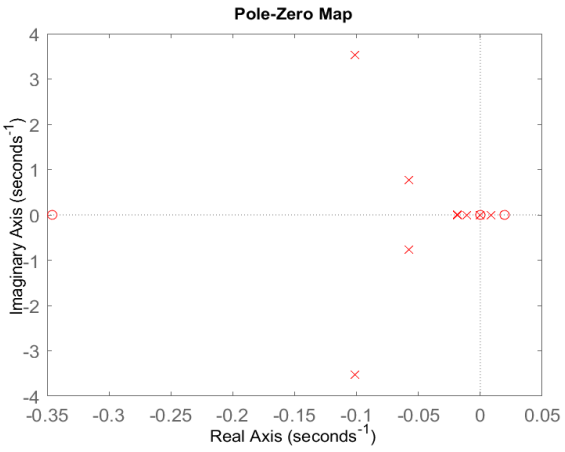

Figure 7. Pole zero plot

4.2 Controller Implementation

The AHV 6DOF linear model is used for the control design considering state feedback development using pole placement. AHV model given by (22)-(26) is used for the open loop simulation, with the linear aero–dynamic coefficients using (13)-(18) and the propulsion engine model by (19) is incorporated in the simulation, and the state feedback with pole placement using (31)-(35), is used for the dynamic stability implementation.

The linear AHV state space model output given by (26) is simulated for the control to be implemented for the corresponding input given by (25). Closed loop simulation is performed for the output A_n, and a comparison of the open and closed loop is shown in Figure 8.

The open-loop and closed-loop response analysis of AHV is shown in Figure 8. It illustrates the stability with closed-loop design and hence shows convergence in the output generated via the pole placement design and state feedback technique.

The gain value $\boldsymbol{K}$ for the AHV closed-loop perfor–mance is determined using pole placement and is given by (35),

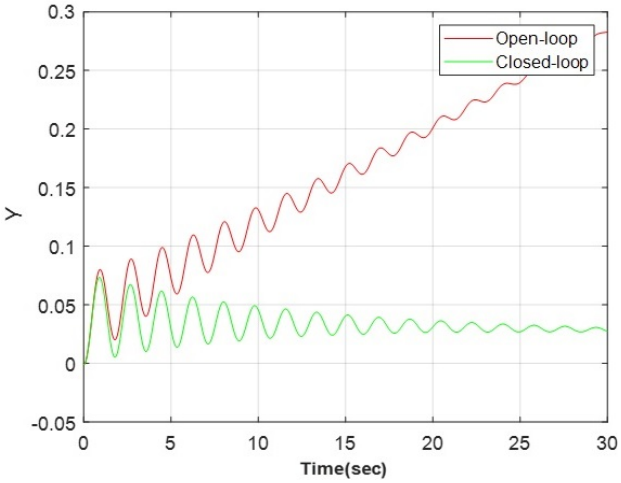

Figure 8. The output response of Y for open and closed loop

$$K = \begin{bmatrix} -0.1014 + 3.5328i \\ -0.1014 - 3.5328i \\ -0.0089 + 0.0000i \\ -0.0111 + 0.0000i \\ -0.0580 + 0.7680i \\ -0.0580 - 0.7680i \\ -0.0184 + 0.0068i \\ -0.0184 - 0.0068i \\ 0.0000 + 0.0000i \\ 0.0000 + 0.0000i \end{bmatrix} \tag{35}$$

In MATLAB, the state feedback technique is used to implement the control law design, as shown in Fig. 8. The aileron and rudder desired deflection is controlled using the controller for the AHV linear model using feedback design and corresponding deflection in terms of a controller response is obtained. AHV model is simulated using MATLAB software for dynamic simulation.

The dynamic response for the AHV model is perfor–med with different controller implementations using the block diagram, as illustrated in Figure 4 and Figure 9.

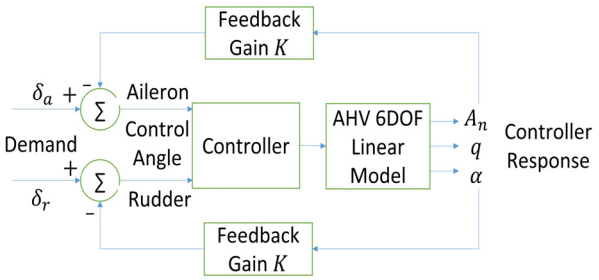

Figure 9. Feedback with controller design

Figure 10 represents the controller design imple–mentation for output A_n, and for δ_a deflection, the PI controller generates better response time due to less overshoot to PID, and for δ_r deflection PI controller gives better response and fast settling time in compa–rison to PID. Figure 11 shows the controller design for output q, and for δ_a deflection, the PID controller generates a better response and faster settling time, and for δ_r deflection, the PID controller gives a better res–ponse and fast settling time. Figure 12 shows the controller design for output α, and for δ_a deflection, the PID controller generates a better and fast response with faster settling time, and for δ_r deflection, the PID controller shows a fast response with fast settling time.

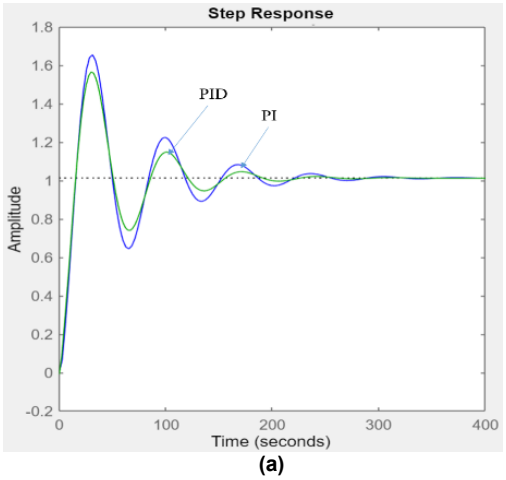

(a)

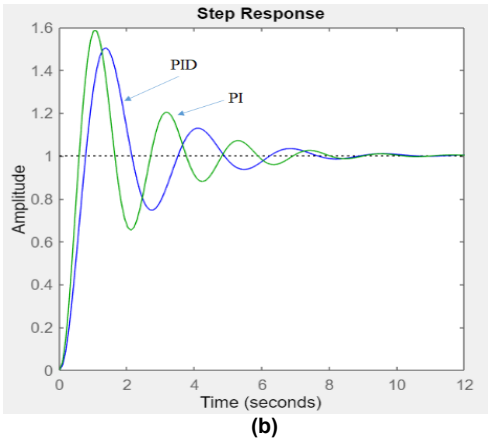

(b)

Figure 10. Response to controller design for output A_n for (a) δ_a deflection and (b) δ_r deflection

The comparison of the implemented controller with other AHV works carried out in the open literature is presented in Table 1 and shows that the controller design for the selected Mach number, M=5 provides a better response than other designs. The PID design pre–sented here finds a better control design in comparison to [2], [6]. The control design presented for the system matrices **A**, **B**, **C**, and **D** from (24)-(26) finds difficulty as the controller order is of higher order, and it's difficult to reduce and then design the control law.

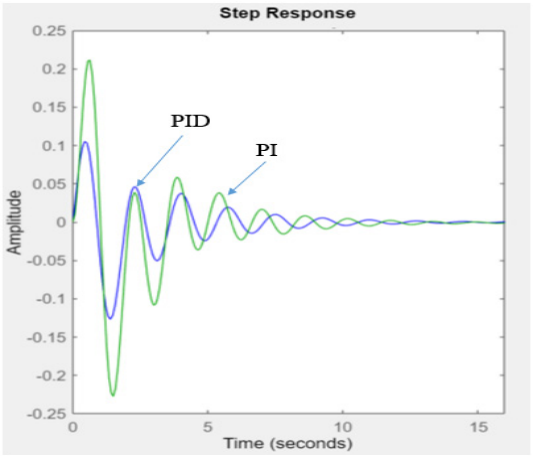

(a)

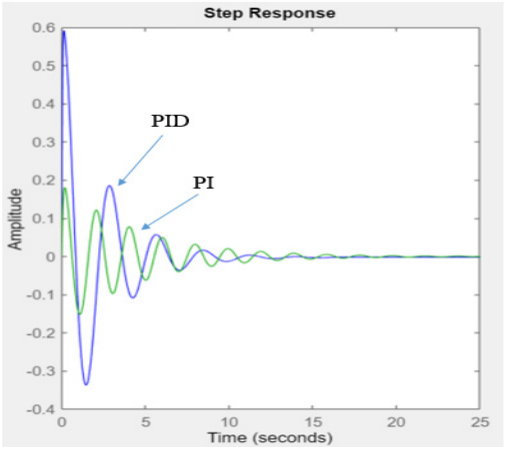

(b)

Figure 11. Response to controller design for output q for (a) δ_a deflection and (b) δ_r deflection

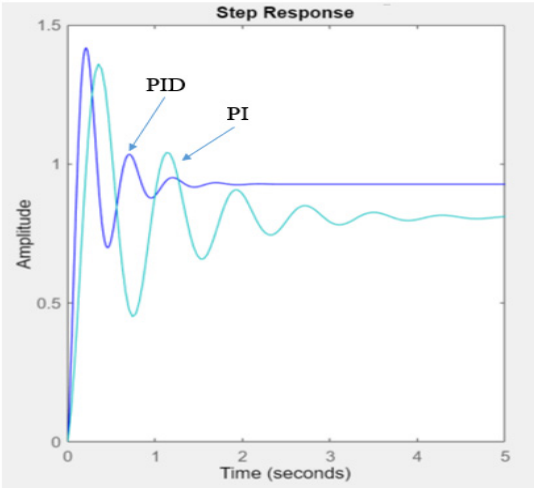

(a)

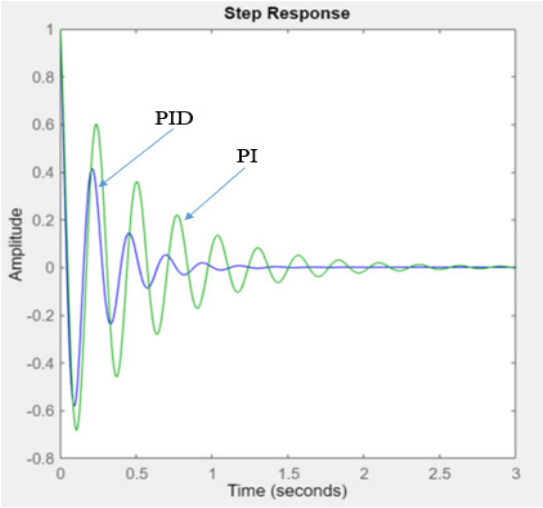

(b)

Figure 12. Response to controller design for output α for (a) δ_a deflection and (b) δ_r deflection

Table 1. Comparison of Results

Related Work	Responses for δ_a deflection and δ_r deflection, Stability of A_n, q, α is Stable				
	t_r	t_s	M_p	PI	PID
This work, M=5	1s	3s	6-9%	slow	fast
[2]	Fast	Fast	6-7%	combined	
[6], M=7	0.02s	3s	5-7%	-	PID+PSO
[22], M=4 to 7	-	3.36s	43.4%	-	PID
[23]	4s	9s	9.4%	-	PID

5. DISCUSSION

The AHV 6DOF dynamic linear model is used for this study's analysis and control design. The model uses a linear aerodynamic model with a ramjet and scramjet engine for the propulsion model. The linear model developed is considered for the steady and wing level flight condition operating at the level and straight flight condition for considered velocity M=5 at an altitude of 65000 *ft* (19812 *m*). The linear model is developed as a state space model with states as x, with inputs given by u as δ_a and δ_r and the output y given as A_n, q, and α. as the normal acceleration, pitch rate, and angle of attack of AHV. The model obtained is decoupled from the longitudinal and lateral system interactions. State space system matrices A, B, C, and D are obtained for the AHV model using mathematical modeling.

This linear model is analyzed for the open loop dynamic simulation for the state space developed model of the AHV for the different inputs δ_a and δ_r deflection. The pole-zero plot of the model shows a nonminimum phase for the poles and zeros, which results in system instability. Hence, the control design is implemented using state feedback architecture for the AHV dynamic model. The dynamic stability of the model is investigated, and state feedback control using pole placement is implemented to attain the stability of the model. The open-loop and closed-loop response analysis of AHV shows the stability with closed-loop design, and convergence is seen using the pole placement design and state feedback technique. Using the control system design tool, the state feedback technique is implemented in MATLAB for the control law design. The aileron and rudder desired deflection is controlled using the controller for the linear model using feedback design. The dynamic response for the AHV model is obtained for different controller implemen–tations for the output A_n, q, and α. For the output, PI and PID controllers are designed and compared for better responses for the δ_a deflection and δ_r deflection. The PI controller gives a better response and fast settling time in comparison to PID for A_n. And PID controller generates a better response and faster settling time for δ_r deflection for q. And PID controller design for output α, generates a better and fast response with faster settling time and shows a better response with fast settling time for δ_r and δ_a deflection, respectively, in comparison to the other designs.

6. CONCLUSION

The dynamic AHV model analyzed for the level flight M=5 Mach number for the δ_a and δ_r deflection shows unstable behavior for the A_n, α, and q with the consi–dered flight condition. The pole-zero location show occurrence of a nonminimum phase for the considered flight state, leading to unstable dynamics, resulting in control design. Responses to controller design for the δ_a and δ_r deflection show that PID gives better response and faster settling time for the considered flight condition at M=5 Mach number and in comparison to other designed controllers.

REFERENCES

[1] Duan, H. and Li, P.: Progress in control approaches for hypersonic vehicle, Science China Technological Science, Springer, Vol. 55, pp. 2965–2970, 2012.

[2] Hu, Z. B., Deng, L. X., and Li, B. B.: Design of Air-Breathing Hypersonic Vehicle Control System, Applied Mechanics and Materials, Trans. Tech Publications, Switzerland, Vol. 719–720, pp. 324–329, 2015.

[3] Taylor, C. J., Chotai, A. and Young, P. C.: Non-linear control by input–output state variable feedback pole assignment, International Journal of Control, Taylor & Francis, Vol. 82, pp. 1029-1044, 2009.

[4] Huang, B., Lu, B., Li, Q.: A proportional–integral-based robust state-feedback control method for linear parameter-varying systems and its application to aircraft, Proceedings of the Institution of Mechanical Engineers, Part G: Journal of Aerospace Engineering, Vol. 233, pp. 4663-4675, 2019.

[5] Ma, J. and Gao, Z.: Pole-Placement for Generalized Systems Simultaneous Stabilization, in: *International Conference on Intelligent Computation Technology and Automation*, *IEEE*, Changsha, China, 2008, pp. 413-417.

[6] Amrutha, K. and Kumar, R. H.: PID Tracking Controller for Air-Breathing Hypersonic Vehicle, in: *International Conference on Emerging Trends*

and Innovations In Engineering And Technological Research, IEEE, Ernakulam, India, 2018, pp. 1-6.

[7] Shaughnessy, J. D., Pinckney, S. Z., Mcminn, J. D., Cruz, C. I. and Kelley, M. L.: Hypersonic vehicle simulation model: Winged-cone configuration, NASA Langley Research Center, NASA-TM-102610, United States, 1990.

[8] Keshmiri, S., Colgren, R., and Mirmirani, M.: Six-DOF Modeling and Simulation of a Generic Hypersonic Vehicle for Control and Navigation Purposes, in: *AIAA Guidance, Navigation, and Control Conference and Exhibit*, Colorado, United States, 2006, pp. 6694-6704.

[9] Keshmiri, S., Colgren, R., and Mirmirani, M.: Six DoF Nonlinear Equations of Motion for a Generic Hypersonic Vehicle, in: *AIAA Atmospheric Flight Mechanics Conference and Exhibit*, South Carolina, United States, 2007, pp. 6626-6654.

[10] Keshmiri, S., Colgren, R., and Mirmirani, M.: Development of an Aerodynamic Database for a Generic Hypersonic Air Vehicle, in: *AIAA Guidance, Navigation, and Control Conference and Exhibit*, San Francisco, United States, 2005, pp. 6257-6278.

[11] Singh, R., Prakash, O., Joshi, S., and Jeppu, Y.: Longitudinal Trim and Stability Analysis of Generic Air-Breathing Hypersonic Vehicle using Bifurcation Method, INCAS Bulletin, Vol. 14, pp. 111-123, 2022.

[12] Prakash, O., Singh, R., Joshi, S., Jeppu, Y.: Flight Dynamics Analysis using High Altitude & Mach Number for Generic Air-Breathing Hypersonic Vehicle, in: *AIAA Propulsion and Energy Forum*, Virtual Event, United States, 2021, pp. 3271-3284.

[13] Roskam, J., Lan, C. T.: *Airplane Aerodynamics and Performance*, Darcorporation, Lawrence, Kansas, 2000.

[14] Stevens, B. L., and Lewis, F. L.: *Aircraft Control and Simulation*, Wiley, New York, 2003.

[15] Urakawa, Y.: Application of Limited Pole-Placement Method to State Feedback System, in *IEEE International Conference on Mechatronics*, Kashiwa, Japan, 2021, pp. 1-5.

[16] Williams II, R. L., Lawrence, D. A.: *Linear State-Space Control Systems*, New Jersey, John Wiley & Sons, 2007.

[17] Michiel, H. et al. Hardware and control co-design enabled by a state-space formulation of cascaded, interconnected PID controlled systems, in: *7th International Conference on Optimization and Applications (ICOA)*, Wolfenbüttel, Germany, 2021, pp. 1-6.

[18] Wang, L.: *Implementation of PID Controllers, PID Control System Design and Automatic Tuning using MATLAB/Simulink*, Wiley-IEEE Press, 2020, pp.113-138.

[19] Unser, M.: A Note on BIBO Stability, IEEE Transactions on Signal Processing, Vol. 68, pp. 5904-5913, 2020.

[20] Oppenheimer, M. W., and Doman, D. B.: Control of an unstable, nonminimum phase hypersonic vehicle model, in: *IEEE Aerospace Conference*, MT, USA, 2006, pp. 1-7.

[21] Xu, B., Wang, X., and Shi, Z.: Robust Adaptive Neural Control of Nonminimum Phase Hypersonic Vehicle Model, IEEE Transactions on Systems, Man, and Cybernetics: Systems, Vol. 51, pp. 1107-1115, 2021.

[22] Li, J., Li, D., Wu, G., and Liu, K.: Flight-Propulsion Integration Dynamic Analysis and Adaptive Control of the Hypersonic Vehicle at Wide-Range Mach Numbers, IEEE Access, Vol. 10, pp. 6954-6965, 2022.

[23] Zhang, Y., and Sheng, G.: Design of Fuzzy Neural Network PID Controller for Hypersonic Vehicle, in: *Chinese Automation Congress (CAC)*, Hangzhou, China, 2019, pp. 3627-3631.

[24] Singh, R., Prakash, O., Joshi, S. and Jeppu, Y.: Linear Controller Design for Generic Air-Breathing Hypersonic Vehicle for different Control Inputs in: *International Conference for Advancement in Technology (ICONAT)*, *IEEE* Goa, India, 2022, pp. 1-6.

[25] Simone, M. C. D., and Guida, D.: Control Design for an Under-Actuated UAV Model, FME Transactions, Vol. 46, pp. 443-452, 2018.

[26] Petrovic, A., Lomovic, M., Ristanovic, M., and Petrovic, A.: Modelling, Simulation and Control of Desalination Plant with a Liquid Jet Ejector, FME Transactions, Vol. 46, pp. 530-536, 2018.

NOMENCLATURE

u, v, w	Velocity along the body axis
$\dot{u}, \dot{v}, \dot{w}$	Accelerations along the body axis
p, q, r	Angular velocities
$\dot{p}, \dot{q}, \dot{r}$	Angular rates
F_{ax}, F_{ay}, F_{az}	Aerodynamic forces
L_a, N_a, M_a	Aerodynamic moment
ϕ, θ	Roll angle, and a Pitch angle
m, h	Mass and altitude
c_1 to c_9	Constants moments of inertia
V	Velocity
α, β	Angle-of-attack and sideslip angle
M	Mach number
C_L	Lift coefficient
C_D	Drag coefficient
C_m	Pitching moment coefficient
C_Y	Side force coefficient
C_l	Rolling moment coefficient
C_n	Yawing moment coefficient
L, D, Y	Lift, drag, and side force
L_a, M_a, N_a	Rolling, pitching, and yawing moment
$C_{L,\alpha}, C_{L,\delta e}$	Increment derivatives
δ_e	Elevator deflection
δ_a	Aileron deflection
δ_r	Rudder deflection
A_n	Normal acceleration
T	Thrust

Acronyms

AHV	Air-breathing Hypersonic Vehicle
GHV	Generic Hypersonic Vehicle
DOF	Degree-of-freedom
SSTO	Single Stage To Orbit
FCS	Flight Control Systems
PI	Proportional Integral
PD	Proportional Derivative
PID	Proportional-Integral-Derivative
PLA	Pilot-lever-angle
LTI	Linear Time Invariant
BIBO	Bounded Input Bounded Output
RHS	Right-hand-side *s*-plane

ДИЗАЈН УПРАВЉАЊА КОРИШЋЕЊЕМ ПИД-А СА ПОВРАТНОМ СПРЕГОМ СТАЊА ЗА ХИПЕРСОНИЧНУ ЛЕТЕЛИЦУ СА AIR-BREATHING ПОГОНОМ

Р. Синг, О. Пракаш, С. Џоши

У раду се користи техника повратне спреге стања да би се обезбедио метод пројектовања управљања за динамички линеарни модел са 6 степени слободе (ДОФ) хиперсоничне летелице са Air-Breathing погоном (АХВ). Развијен је линеарни модел АХВ са моделом простора стања за симулацију отворене петље за ниво лета са Маховим бројем 5 и висином од 65000 фт (19812 м). Анализирана је динамичка стабилност АХВ-а и имплементирана је повратна спрега стања са методом постављања полова за дизајн контролера. Приказани су динамичка стабилност, одзив и поређење за ПИ и ПИД контролер за отклон крилаца δa и отклон кормила δr за АХВ линеарни модел.